HYPERNUCLEAR PHYSICS

POLARIZATION EFFECTS IN EXCLUSIVE HYPERON PRODUCTION REACTIONS

F. Balestra, S. Bossolasco, M.P. Bussa, L. Fava, L. Ferrero, R. Garfagnini, A. Grasso, A. Maggiora, D. Panzieri, G. Piragino, F. Tosello, and G. Zosi
Istituto di Fisica "A. Avogadro" and INFN, Torino, Italy

L.C. Bland, S. Choi, M. Dzemidzic, W.W. Jacobs, J. Shao, and S.E. Vigdor
Indiana University and Indiana University Cyclotron Facility, Bloomington, Indiana 47408

Y. Bedfer, R. Bertini, F. Brochard, J.C. Faivre, and D. Gill
Laboratoire National Saturne, Saclay, France F-91191

L. Barabash, K. Bunyatov, I.V. Falomkin, V. Ivanov, G.B. Pontecorvo, V.I. Travkin, A. Volkov, and B. Zalikhanov
JINR, Dubna, Russia 101000

E. Grosse, P. Senger, and M. Waters
GSI, Darmstadt, Germany D-6100

J. Foryclarz and P. Salabura
Institute of Physics, Krakow, Poland PL-30-059

A. Brenschede, W. Kuhn, and H. Pfaff
Physicalisches Institut, Giessen, Germany D-6300

K. Garrow and J. Stroth
Institut fur Kernphysik, Frankfurt, Germany D-6000

The DISTO collaboration was formed to investigate polarization effects in the exclusive hyperon production reactions, $\vec{p}p \rightarrow pK^+\vec{\Lambda}$ and $pK^+\vec{\Sigma}^0$, induced by polarized protons up to 2.9 GeV at Laboratoire National Saturne.[1] The reactions are induced on a liquid hydrogen (LH_2) target, placed at the center of a large-gap C-magnet, and all outgoing charged products (p, K^+ and the Λ daughters p, π^-) within $\pm 45°$ horizontally and $\pm 15.5°$ vertically of the beam are tracked through a series of scintillating fiber (SF) and multiwire proportional (MWPC) chambers. The measurements are kinematically complete for both reactions, even without detecting the photon resulting from the $\Sigma^0 \rightarrow \Lambda + \gamma$ decay. Momentum resolution of $\sim 1\%$ for the outgoing proton and kaon will provide the missing mass resolution needed to distinguish Λ from Σ^0 production. The outgoing hyperon polarization will be determined in each case from the weak decay asymmetry of the Λ.[2] The comparison of analyzing powers, polarizations, and polarization-transfer coefficients for Λ and Σ^0 production is expected to place strong constraints on the mechanism for

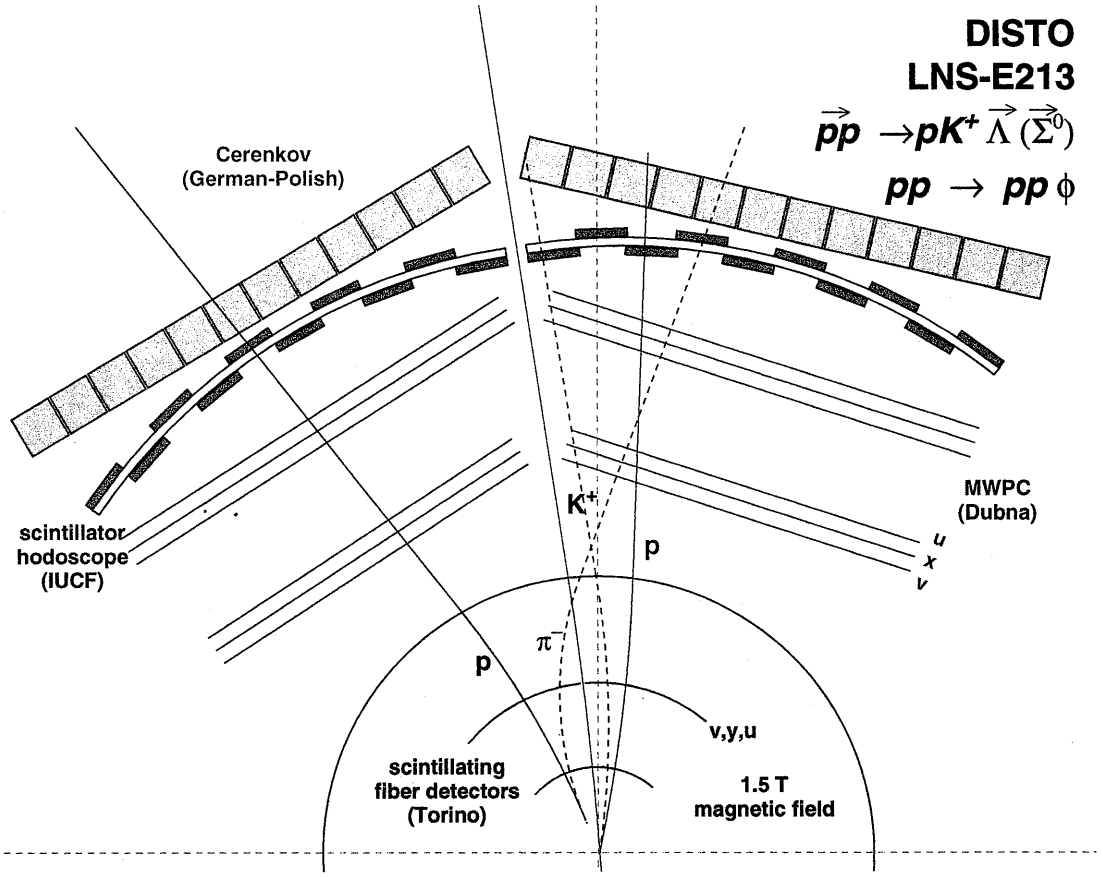

Figure 1. Layout of the DISTO detectors shown in plan view with a simulated pp $\rightarrow$ $pK^+\Lambda$ event. The target and all fiber chambers are embedded in a magnetic field; the inner MWPC's are positioned just beyond the magnet's poletips.

production of open strangeness near threshold.[3,4] The same apparatus can be used as well for the study of the *hidden* strangeness channel pp $\rightarrow$ ppϕ.

Considerable progress has been made during the past year on the beam line and detector setup for the experiments, on the design of suitable triggers, and on the acquisition and analysis software. The full complement of SF chambers (constructed by the Torino group) and an array of water Cerenkov counters (supplied by the German and Polish collaborators) have been added to the previously-installed IUCF plastic-scintillator hodoscope. A curved, thin-walled carbon-fiber vacuum pipe has been fabricated to transport the beam protons from shortly after the LH_2 target cell to the beam dump. An attempt by the Dubna group to construct wire chambers of cylindrical geometry (concentric with the SF and hodoscope), with a small hole in the center for beam passage, did not succeed, and we are presently awaiting delivery of replacement planar MWPC's. The schematic layout of the final detector setup is shown in Fig. 1. In the meantime, we had a successful test run in May 1995 utilizing borrowed planar MWPC's of much smaller area (and only two, rather than three, planes of position measurement apiece) than the ones to be supplied from Dubna.

The SF readout scheme, based on Hamamatsu 80-anode phototubes and LeCroy PCOS III electronics, has not met our original design goals. The efficiencies for minimum-ionizing particles are lower (~80% per plane) and the crosstalk among nearby anodes higher than expected. These problems, if they persist, have serious implications for the hardware and software triggers planned for the experiment and for the retracking algorithm to be used for multi-particle event reconstruction. The hardware (Level 1) trigger is intended to select, on the basis of SF and hodoscope hit multiplicities, events with at least four charged prongs. However, we will have to relax the fiber multiplicity requirement to allow for inefficiencies, and this, combined with crosstalk, will increase the background trigger rate. The Level 2 (software) trigger, to be implemented in four RISC 5000 CPU's, was originally designed to exploit the appreciable separation between hyperon production and decay vertices by rejecting events consistent with four tracks diverging from a *common* vertex. But the substantial number of missing and extra hits now expected at the SF chambers makes it difficult to identify unambiguous tracks with sufficient processing speed for the Level 2 trigger.

The IUCF group is currently working on the design of a new Level 2 trigger, which will utilize particle-identification information inferred from the recently-installed Cerenkov counters, in place of searching for two separated vertices. In addition to bypassing the SF hit-pattern ambiguities, this approach will allow us to take $pp \rightarrow pp\phi$ (followed by $\phi \rightarrow K^+K^-$, with no appreciable vertex separation) data at the same time as pKY events. The new Level 2 trigger will consist of two basic stages. In the first, two-dimensional pattern recognition will be employed to identify clusters of fired anodes on the SF phototubes that have most likely resulted from a single particle crossing combined with crosstalk, and to select for each cluster the most probable centroid fiber at which the particle actually crossed the SF chamber. The multiplicity of such clusters, as well as of clusters recorded on the MWPC's, will be checked for consistency with expectations for pKY events. This multiplicity check should be effective in rejecting two-charged-prong events that have passed the (relaxed) Level 1 trigger by virtue of fiber crosstalk and particles falling in the small overlap regions between adjacent x-elements at the scintillator hodoscope. The second stage of the Level 2 software will reject a majority of events that include an energetic π^+ or a π^- more energetic than expected from Λ decay. This should greatly reduce the dominant background source surviving the first stage, namely, $pp \rightarrow pp\pi^+\pi^-$ reactions. The fast pions will be identified by the combination of large Cerenkov-counter pulse height and relatively low momentum. The momentum will be reconstructed crudely, but very quickly, from the MWPC hits in the immediate vicinity of the fired Cerenkov element, under the assumption of a track originating at the target center and traversing a uniform field inside an effective field boundary. Simulations show that we should be able to achieve ~10% momentum resolution under these simplified assumptions, sufficient to produce the particle identification loci seen in Fig. 2.

Incorporation of SF hits into the momentum determinations will then be done only in the full event-reconstruction software. As a first step toward that software, the IUCF group has written a simplified retracking program intended for analysis of two-charged-prong events. Here, we include in the track reconstruction only chambers where a single cluster was recorded on at least two planes. The minimum information needed then to

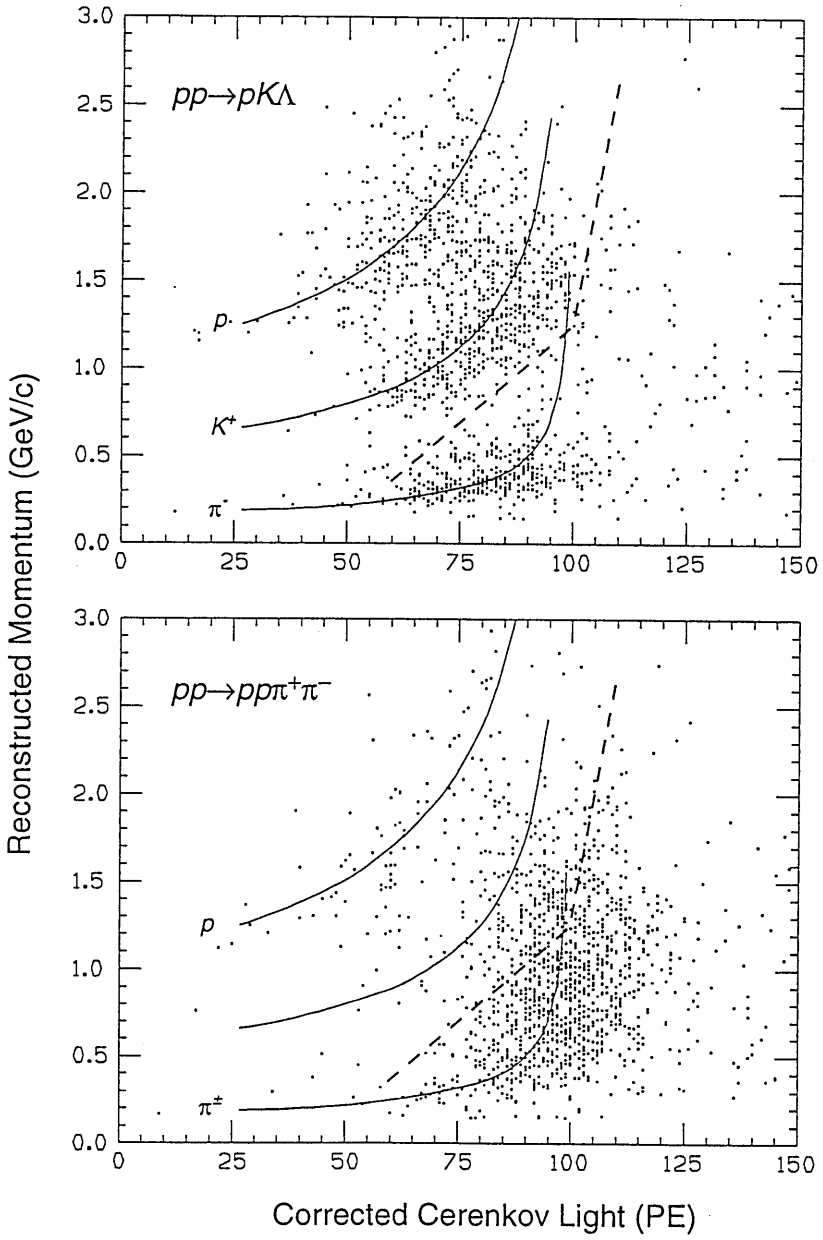

Figure 2. Simulated particle-identification spectra obtainable with the proposed Level 2 trigger algorithm. The Cerenkov-counter pulse heights are corrected, event-by-event, for path-length differences inferred from the MWPC ray-tracing. The solid curves indicate the pulse-height variations with momentum expected for perfect reconstruction. Events including positively charged particles falling to the right of the dashed lines would be rejected in the Level 2 trigger. Further suppression of $pp\pi^+\pi^-$ background could be effected by rejecting negatively charged tracks with corrected Cerenkov pulse height above 100 photoelectrons.

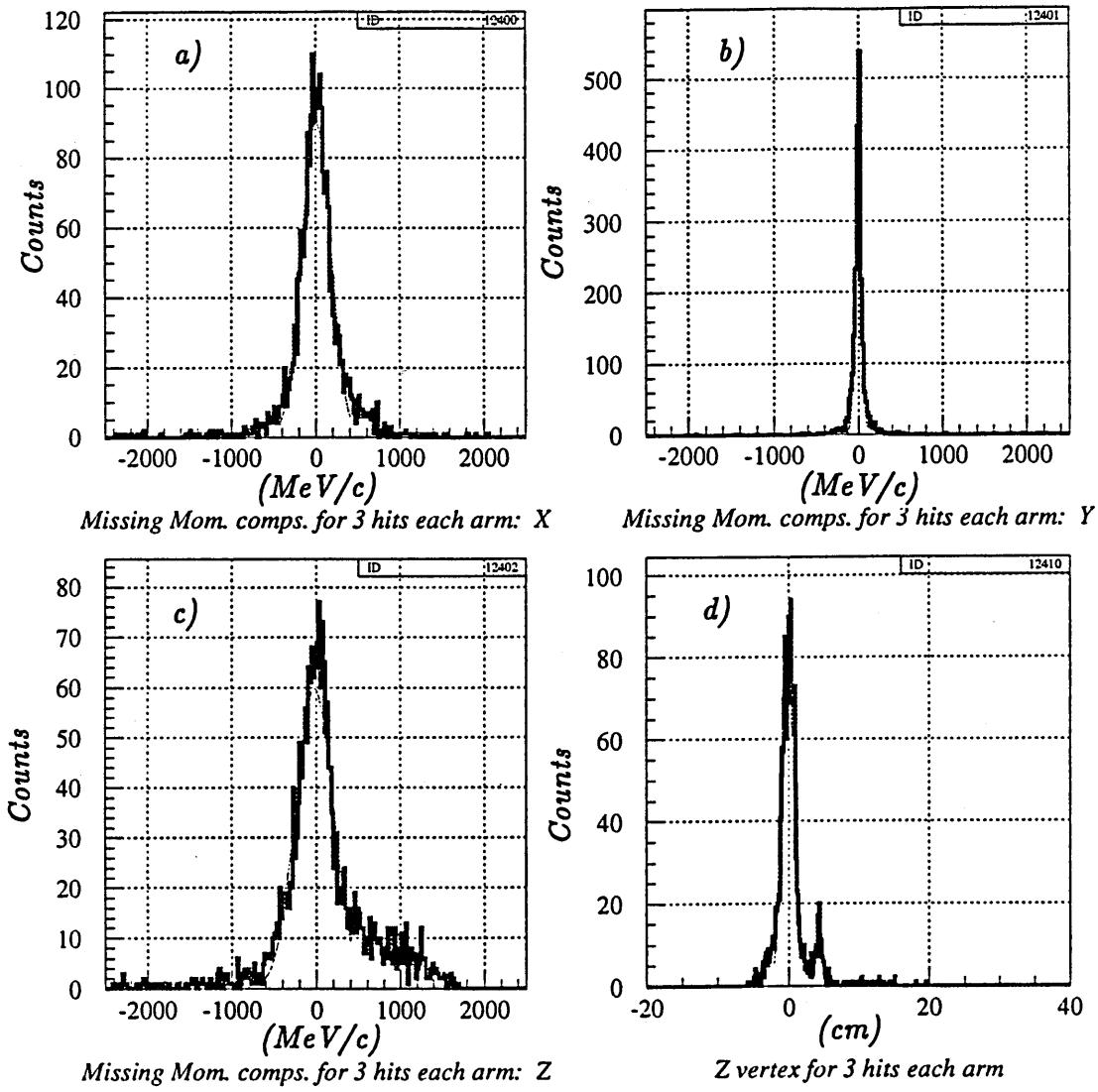

Figure 3. Spectra of missing momentum components (a-c) and of longitudinal vertex coordinate (d) reconstructed from data acquired with a hardware trigger designed to select hodoscope hits consistent with p-p elastic scattering at 1.6 GeV bombarding energy.

deduce particle momenta and the event vertex location are hits on at least three chambers on one arm and at least two chambers on the other arm. This software is currently being tested on p-p elastic scattering and $pp \rightarrow d\pi^+$ data acquired in May 1995 at 1.6 GeV and 2.9 GeV bombarding energies. It will be used subsequently to search for $pp \rightarrow pn\pi^+$ events among the data collected, and as a starting point for development of multi-particle retracking to analyze 2.9 GeV data obtained with candidate Level 1 triggers in the May run.

Representative results from the ongoing analysis of 1.6 GeV p-p elastic scattering events are shown in Fig. 3. The reconstructed momentum resolution is extremely sensitive to the geometry parameters for all the chambers, and is still far from optimized. On the

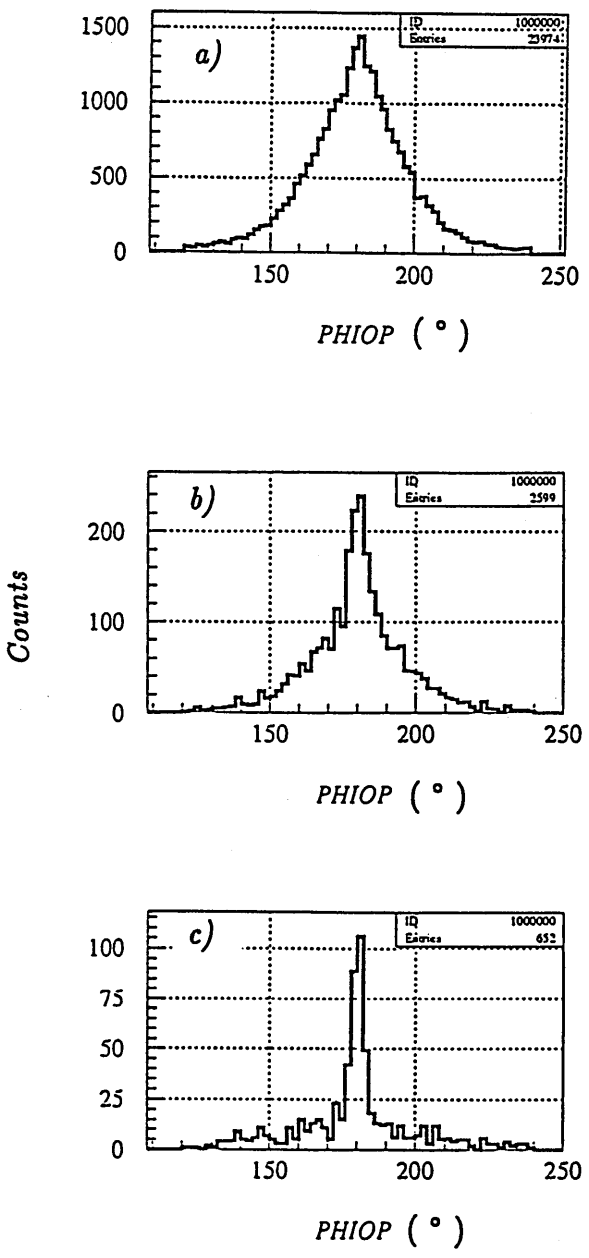

Figure 4. Spectra of the reconstructed azimuthal opening angle (coplanarity) for events acquired at 1.6 GeV with a hardware trigger selecting hodoscope hits consistent with the pp $\rightarrow$ dπ^+ reaction. The spectra are shown with (a) no software cuts, (b) π^+ identification in a right-arm Cerenkov counter, and (c) the additional requirement of an energy deposition at least 25% greater than that for minimum-ionizing particles in the left-arm hodoscope element corresponding to the maximum kinematically-allowed deuteron angle. The pp $\rightarrow$ dπ^+ events fall in the peak centered at 180°.

other hand, the reconstructed vertex resolution is already good: the spectrum in Fig. 3(d) shows the majority of events originating from within the 2 cm length of the LH_2 cell, but a clear secondary peak is seen at the location of the entrance window to the carbon-fiber beam-dump pipe. Figure 4 shows analysis results for pp $\rightarrow$ dπ^+ events acquired also at 1.6 GeV, with a hardware trigger designed to eliminate elastic scattering. The coplanarity

peak expected for the 2-body pion production emerges very clearly when the spectrum is gated by appropriate cuts on other reconstructed kinematic variables.

Further runs and developments planned for Fall 1995 should bring the DISTO experiment to the point of production running in 1996.

1. A. Maggiora, *et al.*, in *Proc. Intl. Workshop on Flavour and Spin in Hadronic and Electromagnetic Interactions*, ed. F. Balestra, *et al.* (Italian Physical Society, Bologna, 1993) p. 111.
2. W.W. Jacobs, *et al.*, in *Proc. Eighth Intl. Symposium on Polarization Phenomena in Nuclear Physics*, eds. E.J. Stephenson and S.E. Vigdor (AIP Conf. Proc. No. 339, 1995) p. 476.
3. J.M. Laget, Phys. Lett. **B259**, 24 (1991), and private communication.
4. S.E. Vigdor, in *Proc. Intl. Workshop on Flavour and Spin in Hadronic and Electromagnetic Interactions*, ed. F. Balestra, *et al.* (Italian Physical Society, Bologna, 1993) p. 317.